

# Technical Report

## TR-13-24

### **Self-diffusion and impurity diffusion of hydrogen, oxygen, sulphur and phosphorus in copper**

Hans Magnusson, Karin Frisk  
Swerea KIMAB AB

December 2013

**Svensk Kärnbränslehantering AB**  
Swedish Nuclear Fuel  
and Waste Management Co  
Box 250, SE-101 24 Stockholm  
Phone +46 8 459 84 00



ISSN 1404-0344

SKB TR-13-24

ID 1415328

# **Self-diffusion and impurity diffusion of hydrogen, oxygen, sulphur and phosphorus in copper**

Hans Magnusson, Karin Frisk  
Swerea KIMAB AB

December 2013

This report concerns a study which was conducted for SKB. The conclusions and viewpoints presented in the report are those of the authors. SKB may draw modified conclusions, based on additional literature sources and/or expert opinions.

A pdf version of this document can be downloaded from [www.skb.se](http://www.skb.se).

## Abstract

A study on the mobility of hydrogen, oxygen, sulphur, and phosphorus in copper has been made. In addition, the self-diffusion of copper has also been studied. Literature data has been reviewed, and used to evaluate the temperature expressions of the diffusion coefficients of these elements in copper. The interstitial elements oxygen and hydrogen have been described by a single temperature expression in the whole temperature range, whereas the substitutional elements copper, sulphur, and phosphorus have been modelled according to lattice diffusion at high temperatures and grain boundary diffusion at low temperatures.

Sulphur, phosphorus, and copper are believed to be nearly immobile within the crystalline grains at low temperature, even for time periods up to 100,000 years. On the other hand, in the grain boundaries these elements can diffuse and an upper limit estimate of the possible diffusion distance has been made. At room temperature sulphur can diffuse up to 5 cm for 100,000 years, whereas both phosphorus and copper requires more than 1,000 000 years to diffuse the same distance. The oxygen atom shows a similar mobility, although it is interstitially diffusing through the grains. However, since both oxygen and sulphur have a very low solubility any measureable mass transport of these elements will never take place at low temperatures. They will instead form oxides and sulphides in the material.

Hydrogen is a mobile element, and will be able to diffuse through 5 cm of copper during a time period of 1,000 years at room temperature. The diffusion of hydrogen in copper is experimentally well studied down to room temperature. By combining the evaluated hydrogen diffusion coefficient with the thermodynamically calculated hydrogen content in solid solution the permeability of hydrogen can be explained. This can be used to explain the mass-transport of hydrogen for different times, temperatures, and hydrogen activities (pressures).

# Contents

<b>1</b>	<b>Introduction</b>	7
<b>2</b>	<b>Diffusion mechanisms and diffusion distance</b>	9
2.1	Introduction to diffusion	9
2.2	Experimental evaluation of diffusion	9
2.3	Grain boundary diffusion	11
2.4	Diffusion profiles and random-walk	12
<b>3</b>	<b>Evaluation of diffusion coefficients in copper</b>	13
3.1	Cu-H	13
3.2	Cu-O	14
3.3	Cu-S	16
3.4	Cu-P	18
3.5	Cu-Cu	18
<b>4</b>	<b>Extrapolation of diffusion data to low temperatures</b>	23
<b>5</b>	<b>Relating time and temperature to a diffusion distance</b>	29
5.1	Grain boundary diffusion and lattice diffusion	29
5.2	Sulphur and phosphorus diffusion	30
5.3	Hydrogen and oxygen diffusion	31
<b>6</b>	<b>Discussion</b>	33
<b>7</b>	<b>Conclusions</b>	35
	<b>References</b>	37

# 1 Introduction

Oxygen-free phosphorus copper (OFP-copper) is chosen as canister material for spent nuclear fuel. The canister's barrier and its structural integrity requires the OFP-copper to have sufficient material properties, such as creep ductility and resistance to corrosion (SKB 2010b). The main properties of the canister in order to fulfil its barrier function are sufficient creep ductility and shell thickness. The thickness of the copper shell is 5 cm OFP-copper. The compositional limits of OFP-copper are based on the experiences of how ppm levels of elements influences the material properties of the material (SKB 2009). The limits are built on standards and additionally specified to hydrogen less than 0.6 ppm, oxygen lower than 5 ppm, sulphur less than 12 ppm, and phosphorus 30–100 ppm (SKB 2006, 2009, 2010b).

To evaluate the possible influence of impurity or alloying elements for copper at service conditions the mobility of these elements must be clarified. By determining the mobility of the elements it can be identified what kind of mechanism or reaction that can possibly occur at these conditions. For instance, a corrosion reaction such as hydrolysis of water or corrosion of copper in sulphide environment can produce hydrogen (SKB 2010a), which can possibly diffuse into the material and influence the properties of the canister material. Another example is the role of phosphorus on the creep properties of copper. Phosphorus has shown a positive influence on creep strength and ductility (Andersson-Östling and Sandström 2009, Wu et al. 2013), where the mobility of the dislocation is put in relation to the mobility of the phosphorus atom. Finally, creep modelling and cavity growth modelling are related to the mobility of vacancies in lattice and in grain boundary which are proportional to the self-diffusion rate of copper. It is important to clarify the atomic mobility at low temperatures in order to determine the rate of reactions taking place in OFP-copper.

An obvious requirement to experimentally evaluate the mobility, or the diffusion coefficients, is that diffusion must have been allowed to take place. Sufficient time at a given temperature will allow for chemical diffusion of the impurity atom or self-diffusing atom. The diffusion coefficients can then be evaluated based on the diffused distance at a certain time and temperature. The absence of experimental studies of diffusion at low temperatures is an indication of the low diffusivities at these conditions. An exception is the high mobility of the small hydrogen atom, which has been studied down to room temperature. However, the long service time for the canister material to be used for the spent nuclear fuel could allow measurable diffusion distances at low temperatures. In order to estimate the diffusion coefficient at these temperatures extrapolations are needed. This will require information on the mechanism of diffusion to make a reliable extrapolation.

The aim of the present work is to evaluate the diffusion coefficient for copper self-diffusion and for hydrogen, oxygen, sulphur and phosphorus impurity diffusion in copper. This diffusion data will be used to estimate typical diffusion distances at low temperature service. The possible influence of different mechanisms related to diffusion will be discussed. A limitation in the present work is that only diffusion in the FCC phase will be considered, and not in the complex phases such as oxides and sulphides. The FCC phase (face centric cubic) represents copper in its standard crystallographic structure. In addition, only low concentrations of the diffusing elements are considered.

## 2 Diffusion mechanisms and diffusion distance

### 2.1 Introduction to diffusion

Atoms will diffuse in a material in equilibrium even though nothing seems to happen from a macroscopic point of view. In order to study and quantify this diffusion phenomenon, a measureable concentration gradient is needed. In the case of pure metal a radioisotope is often used to measure the tracer diffusion coefficient. If the tracer is chemically the same as the host metal it will be a self-diffusion study. In the cases when the tracer is chemically different to the host metal it will be a study of impurity diffusion.

Diffusion takes place through the movement of point defects in the crystalline lattice. Different types of point defects will give rise to different mechanisms of diffusion. The most common mechanism for diffusion of larger atoms in metals at high temperatures is the vacancy mechanism. This mechanism is illustrated in Figure 2-1a. Vacancy diffusion takes place when substitutionally dissolved atoms jump to an unoccupied lattice site (vacancy). Substitutional diffusion can also occur in interaction with other crystalline defects, such as grain boundaries and dislocations. It is generally accepted that these defects can act as fast diffusion paths in the material. Grain boundary diffusion is an important mechanism for polycrystalline materials at low temperatures.

Another type of diffusion is interstitial diffusion, as shown in Figure 2-1b. It occurs when an interstitial small atom, such as hydrogen or oxygen, moves from one interstitial site to another neighbouring interstitial site. Since this method will require a local distortion of the crystalline lattice the diffusing atom has to be small in size. The diffusing interstitial atom will not have to wait for any neighbouring vacancy, and the interstitial diffusion is typically quite fast compared to substitutional vacancy diffusion.

### 2.2 Experimental evaluation of diffusion

The experimental studies of impurity diffusion and self-diffusion mainly involve three steps. First, the diffusing species is introduced to the specimen. This can be on the surface of the material if the evaluation is to study the in-diffusion of the element. It can also be a material equilibrated with a high content of the solvent, if the study concerns outgassing of the element. The second step is to heat treat the specimen so that the element will diffuse into or out from the material giving rise to a concentration gradient in the material. Finally, the mass-transfer due to diffusion is measured and the diffusion coefficient can be evaluated. Some common techniques will be briefly reviewed in this work, although further reading can be made elsewhere (Murch and Nowick, 1984, Neumann and Tuijn 2009).

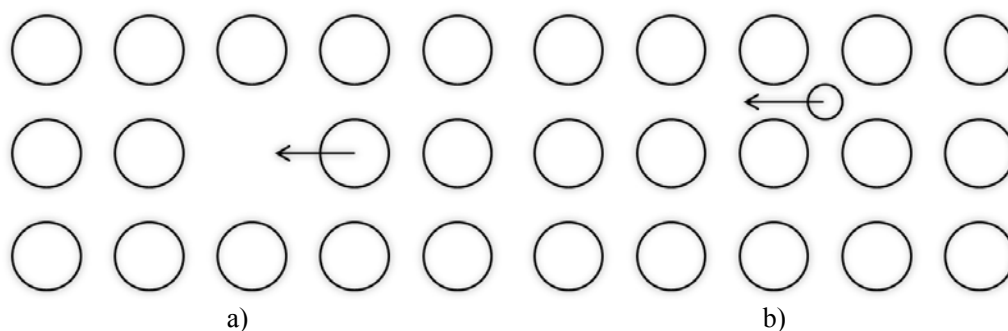


**Figure 2-1.** a) Vacancy diffusion of substitutional elements b) interstitial diffusion of small atoms.

A common procedure, especially for metallic elements, is to use the tracer section technique, as illustrated in Figure 2-2. An isotope of the impurity element is introduced on one side of the sample. The radiotracer can be deposited by different techniques such as evaporation, electrochemical methods, sputtering, etc. The sample is then annealed for some time and at a certain temperature. The specimen is then sectioned into smaller samples in order to determine the concentration of the isotope in each section and thereby producing a penetration profile of the isotope. The activity of the isotope is registered by a scintillation counter. The possibility to measure diffusion coefficients at low temperatures depends on several different factors. Thinner material removal in the sectioning will give a higher resolution of the radiotracer penetration profile. This is needed for low-temperature measurements of diffusion coefficients, and especially when using isotopes with a limited half-life giving little time for specimen annealing. Macrosectioning techniques can be precision lathes and microtomes, with a resolution in the  $\mu\text{m}$ -range. Microsectioning techniques are chemical dissolution, or electrochemical removal of anodised layers, giving down to nm-range resolution. An even higher resolution is to use ion-beam sputtering to measure radiotracer material, or using mass-spectrometer (for instance by secondary ion mass spectrometry, SIMS).

The diffusion coefficient of lighter elements, which are often in the form of gaseous species, can be determined based on the rate of gassing or degassing of thin metal foils. The amount of the element in the foil can be registered by mass changes, or resistivity changes. Permeation methods can also be used to study the diffusion through a thin foil, with a high-pressure side and low-pressure side of a metal foil. By measuring the time it takes for the element to emerge at the low-pressure side, the diffusion coefficient can be calculated. Another approach is to evaluate the steady-state flux of atoms, the permeability, in the foil. However, some care has to be taken since some of these methods will yield the product of the solubility and diffusivity which can give uncertainties in the evaluation.

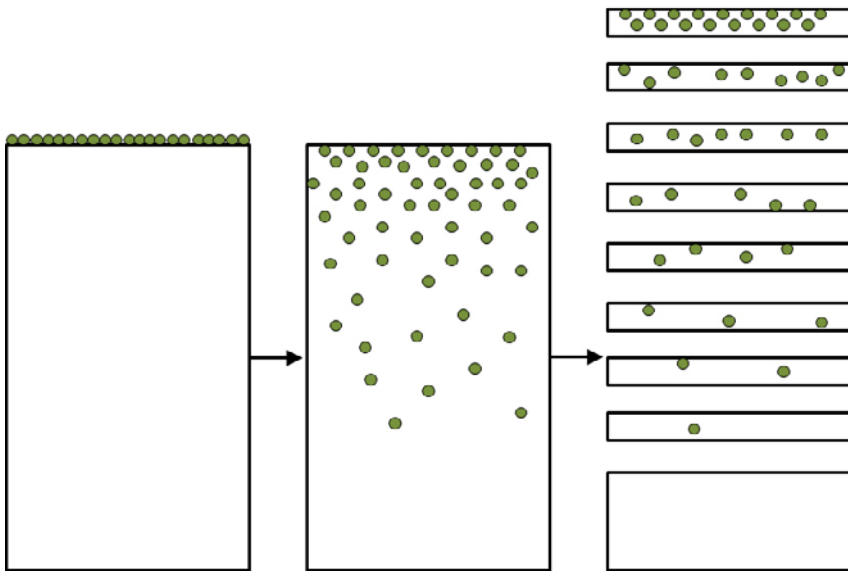


**Figure 2-2.** Schematic illustration of adding radiotracer (isotope) to material, annealing, and sectioning following by counting isotope concentration.

## 2.3 Grain boundary diffusion

Determination of the grain boundary diffusion coefficient is an indirect measurement of the in-diffusion taking place in the grain boundaries of a polycrystalline material. Diffusion of substitutional elements in a polycrystalline material at low temperatures will take place in the grain boundaries alone, or in the grain boundaries plus a minor part of the grains surrounding the fast diffusing boundaries. Grain boundary diffusion, and the influence from lattice diffusion, is often divided into three different regimes (Harrison 1961). These regimes are illustrated in Figure 2-3. The different regimes are distinguished based on magnitude of the lattice diffusion length, estimated as  $\sqrt{D_l t}$ , where  $D_l$  is the lattice diffusion coefficient and  $t$  is the time. For regime C (Figure 2-3c), the diffusion in the material will be located entirely in the grain boundaries. Regime A (Figure 2-3a) is defined as the region where the lattice diffusion distance is much larger than the grain boundary width. In this region there will be a significant overlap of different diffusion paths. For the intermediate case, regime B (Figure 2-3b), diffusion will be somewhat influenced by the grains in close vicinity to the grain boundaries.

An effective diffusion coefficient can be defined, based on both lattice and grain boundary coefficients as suggested by Hart (1957):

$$D_{eff} = f_{GB} D_{GB} + (1 - f_{GB}) D_l \quad (2-1)$$

where  $f_{GB}$  is the fraction of sites belonging to fast-diffusion paths, often estimated as the fraction of the grain boundary width to the grain size. The above equation has been shown to be accurate for two extreme cases: when the distance between the fast-diffusion paths (grain size) is either much smaller or much larger than the diffusion path (Murch and Rothman 1985, Gupta et al. 1978). The first scenario corresponds to regime A type of diffusion, and the latter to the regime C type of diffusion.

The intermediate case is regime B. This is when the lattice diffusing distance is in the same magnitude as the distance between the fast diffusing paths. For this regime there will be some influence of lattice diffusion on the total diffusion in the material, although the main part of the diffusion occurs in the grain boundaries. A general distinction between regime B and regime C type of grain boundary diffusion is that a segregation factor should be included in the type-B grain boundary diffusion. This is motivated by the interaction with the surrounding grains in close vicinity to the grain boundary which increases the overall diffusivity (Mishin et al. 1997). This has been experimentally verified for many different impurity elements diffusing in copper, for instance nickel, silver, and bismuth (Divinsky et al. 2001, 2004, 2007). The low temperature diffusion data in regime C cannot directly be extrapolated to slightly higher temperatures in regime B without the use of this segregation factor  $s$ . In the regime B the product of grain boundary width  $\delta$ , grain boundary diffusion coefficient, and segregation factor is the measured quantity according to  $P^{speB} = s\delta D_{GB}$ . The segregation factor takes typical values 1–1,000, depending on temperature and diffusing element. In regime C, the product of grain boundary width and diffusion coefficient is measured according to  $P^{speC} = \delta D_{GB}$ .

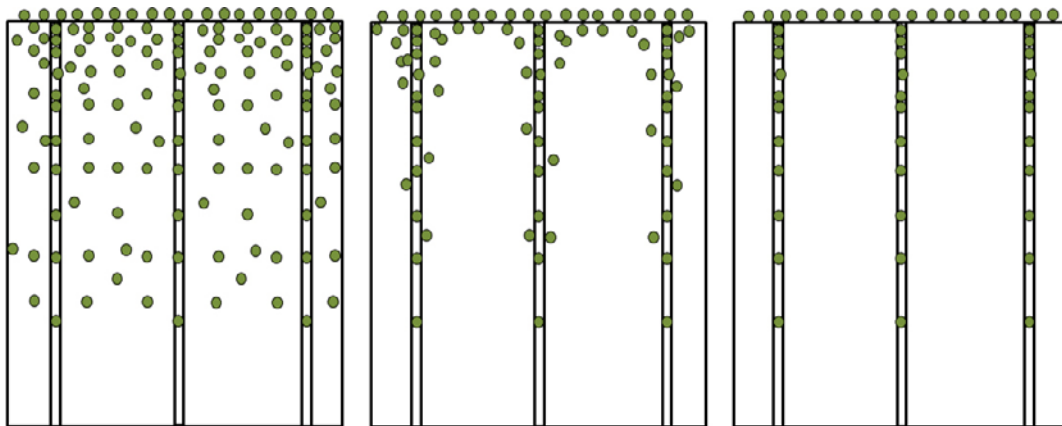


**Figure 2-3.** Schematic figure illustrating the different regimes of grain boundary diffusion, with regime A, B, and C from left to right.



## 2.4 Diffusion profiles and random-walk

The flux of atoms in a one-phase binary system can be expressed by Fick's law, relating the flux of atoms to a diffusion coefficient and concentration gradient according to:

$$J = D \frac{\partial c}{\partial x} \quad (2-2)$$

where  $D$  is the diffusion coefficient,  $c$  concentration, and  $x$  distance. The flux expresses the amount of atoms per unit time passing by a unit area of a plane perpendicular to the  $x$  direction. Based on the law of conservation of mass, Fick's second law can be derived. The equation in one dimension is:

$$\frac{\partial c}{\partial t} = D \frac{\partial^2 c}{\partial x^2} \quad (2-3)$$

For some special cases analytical solutions exist to Fick's second law. The special cases can be well defined boundary conditions, being constant in time. These solutions are true as long as the diffusion coefficient is considered to be independent of concentration. By assuming a fixed concentration at surface  $c_0$ , and a low concentration (in this case zero) far away from the surface the following expressions can be used to estimate the concentration profile:

$$c(t, x) = c_0 \operatorname{erfc}\left(\frac{x}{\sqrt{4Dt}}\right) \quad (2-4)$$

where  $\operatorname{erfc}$  is the complementary error-function and takes a value of 0 for large values.

Another estimate of the diffusion distance is to consider Brownian motion and random walk of atoms in lattice. This approach gives a typical diffusion distance  $\bar{x}$  of atoms in a 2D space according to:

$$\bar{x} = \sqrt{4Dt} \quad (2-5)$$

By comparing Equation (2-4) and (2-5) it can be seen that the typical diffusing distance corresponds to a concentration relative the surface concentration of  $\operatorname{erfc}(1) \sim 15\%$ .

In this work, Equation (2-5) will be used to relate the quantities time, temperature and distance of diffusion. The different mechanisms of diffusion such as grain boundary diffusion, lattice diffusion, and interstitial diffusion, will be expressed by different values of the diffusion coefficient. These diffusion coefficients, and their temperature dependencies, will be evaluated in the present work.

## 3 Evaluation of diffusion coefficients in copper

### 3.1 Cu-H

Measurements on hydrogen diffusivity in copper are mainly based on two different approaches: evaluating the rate of degassing of equilibrated samples, or by measuring the permeating hydrogen through a thin copper foil. The degassing method relies on a copper specimen that is exposed to hydrogen gas at a known pressure and temperature. The specimen is then allowed to degas, and measurements on the release rate of hydrogen or hydrogen isotope is made. The other method relies on evaluating the time and temperature dependence of hydrogen diffusion through a copper membrane. Both the onset of hydrogen permeation and the steady-state flux of hydrogen through the membrane can be evaluated. The hydrogen activity on both sides of the membrane must be well determined.

Low temperature measurements of hydrogen diffusion in copper are mainly studies by Ishikawa and McLellan (1985) and Sakamoto and Takao (1982). Ishikawa and McLellan used an electrochemical approach to introduce hydrogen on one side of a foil. This peak of hydrogen will then diffuse into the material. The breakthrough time is measured at the exit side by emf (electromotive force) changes. Copper with 99.9995% purity was used in the experiments. A conclusion in their work was that no departure from the classical Arrhenius expression occurs for hydrogen diffusion in copper from 1,200K down to 300K. Sakamoto and Takao evaluated the hydrogen solubility and diffusivity in copper for both annealed and cold-rolled copper. The evaluations were made at low temperatures at 19–66°C. The electrochemical permeation method was used with galvanostatic charging of copper. In this work the diffusion data for annealed copper will be used, and thereby avoiding the possible influence of crystalline defects on diffusion. The data for cold-rolled copper show slightly lower diffusivities, and are shown for comparison.

Further studies at intermediate temperatures are by Perkins and Begeal (1972) and work by Caskey et al. (1976). Perkins and Begeal made permeation experiments on polycrystalline copper membranes. The purity was reported to be OFHC commercial purity, which is at least 99.99% purity. Experiments were made in the temperature range of 200–440°C. Caskey et al. determined the hydrogen diffusion coefficient in copper based on evaluated deuterium outgassing. Data used in this work are for commercial grade OF-copper and copper with 99.999% purity. These deuterium measurements are correlated to hydrogen diffusivity by compensating for the difference in mass of the diffusing atoms. This means that the deuterium measurements are multiplied by a factor of two (Butrymowicz et al. 1975). This relation has been discussed by Eichenauer et al. (1965) to be too simple, and rather inaccurate. In the present work, measurements on deuterium will not be used in calculations, although they will be presented for comparison.

High temperature measurements are from older studies by Eichenauer and Pebler (1957) and Eichenauer et al. (1965), and by Katz et al. (1971). Eichenauer and Pebler made hydrogen degassing experiments on copper with unspecified purity. Saturated samples were raised to temperatures of 432–651 °C, and the evolving hydrogen gas content was measured by vacuum gauge measurements. Eichenauer et al. made further experiments, this time on single crystal copper based on 99.999% purity. The same degassing experiments were made, although measurements were made for both hydrogen and deuterium atoms. Katz et al. (1971) studied the diffusion of hydrogen, deuterium and tritium in both copper and nickel. Diffusion coefficients were evaluated based on the rate of hydrogen outgassing. Saturated copper samples were quickly heated by induction and kept in a low-pressure cell. The amount of evolving gas was measured with an ion gauge. Single crystal copper of 99.999% purity was used.

The temperature dependency of the diffusion coefficient of hydrogen in copper has been evaluated based on the measurements by Ishikawa and McLellan (1985), Eichenauer and Pebler (1957), Eichenauer et al. (1965), Katz et al. (1971), Perkins and Begeal (1972), and Sakamoto and Takao (1982). This is shown in Figure 3-1. In general, the whole temperature range 25–1,000°C is quite accurately described by a single temperature function. The temperature expression for hydrogen diffusion in copper is:

$$D_{H,Cu}^{FCC} = 1.74 \cdot 10^{-6} \exp\left(-\frac{42000}{RT}\right) \text{ m}^2/\text{s} \quad (3-1)$$

The diffusion coefficient of hydrogen in copper is evaluated by minimising the sum of all squared errors between the regression line and the experimental values. All experiments have been given an equal weight in the optimisation. Some disagreement exists at low temperature, between the data by Ishikawa and McLellan, and Sakamoto and Takao. Extrapolation of high temperature data fit the values by Sakamoto and Takao better.

### 3.2 Cu-O

Due to the strong interaction between oxygen and copper, the sorption/desorption type of experiments used for hydrogen in copper cannot be applied for oxygen. The studies of oxygen diffusion in copper are based on evaluating the diffusing response of oxygen between two known chemical potentials of oxygen. The chemical potentials are in some cases altered by electrochemical experiments, and thereby relating cell voltage in the galvanic cell to the chemical potential. The corresponding oxygen diffusion and the oxygen removal can be monitored in solid electrolyte galvanic cells by measuring changes in electromotive forces or cell currents. Some of the experimental studies on oxygen diffusivity are based on the total content of diffusing oxygen, and the diffusivities are therefore calculated backwards based on estimated oxygen solubilities. The oxygen solubility has previously been studied as a part of the thermodynamic evaluation of the Cu-H-O-S-P system (Magnusson and Frisk 2013). It will be shown here that some of the diffusion studies have relied on erroneous oxygen solubilities, and have therefore presented unreasonable oxygen diffusivities.

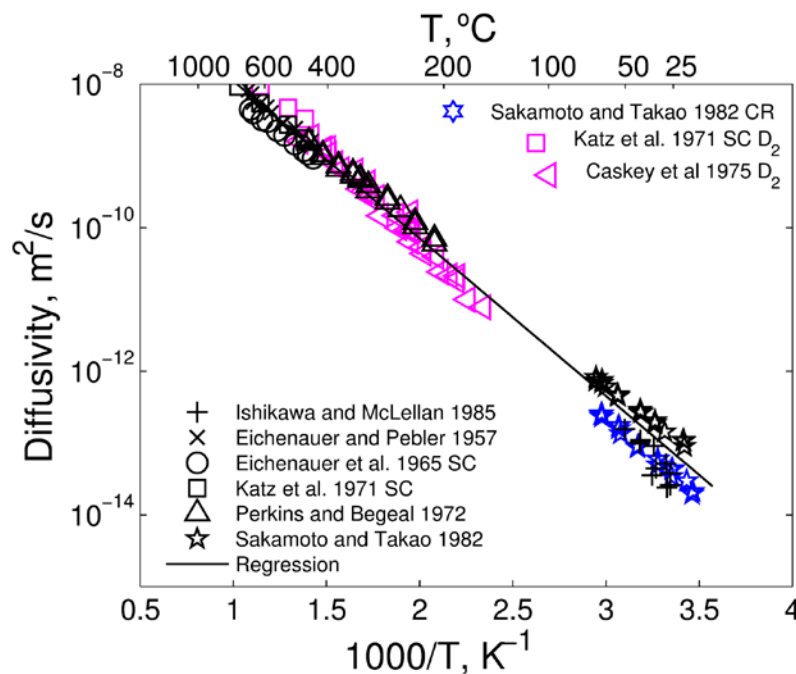


**Figure 3-1.** Evaluated diffusion coefficients for hydrogen in copper, according to references given in the figure. The regression is made for data (presented in black colour) from Ishikawa and McLellan (1985), Eichenauer and Pebler (1957), Eichenauer et al. (1965), Katz et al. (1971), Perkins and Begeal (1972), and Sakamoto and Takao (1982). Data for deuterium gas D<sub>2</sub> are shown as well for comparison (purple colour), and cold-rolled copper denoted CR (blue colour).

Albert and Kirchheim (1981) made direct measurements of oxygen diffusivity in copper based on the measured electromotive forces. Copper of 99.999% purity was used. The oxygen content on the oxygen rich side was maintained by mixed Cu/Cu<sub>2</sub>O material. This allows keeping oxygen in solid solution at the solubility limit of Cu<sub>2</sub>O. The oxygen deficient side was held at low oxygen content with the presence of niobium. Niobium has a very high affinity to oxygen and efficiently lowers the soluble oxygen. The changes in oxygen concentration between the source and sink of oxygen were measured with a galvanic half-cell with a solid electrolyte of ZrO<sub>2</sub>-CaO and reference electrode Cu/Cu<sub>2</sub>O. The change in electromotive force with time is directly proportional to the chemical diffusivity, and the temperature dependence of oxygen diffusion in copper was evaluated. Pastorek and Rapp (1969) determined the diffusivity of oxygen in copper by electrochemical techniques based on potentiostatic and galvanostatic measurements. The ZrO<sub>2</sub>-CaO solid electrolyte was used, with FeO/Fe<sub>3</sub>O<sub>4</sub> reference electrode together with copper of 99.999% purity as electrode.

Ramana Rao and Tare (1972) used a solid electrolyte technique for the determination of the diffusion coefficient of oxygen in copper. By measuring the steady-state current in their electrochemical cell, the steady-state flux of oxygen was evaluated as proportional to the steady-state current. The flux of oxygen depends on both the concentration gradient and the diffusion coefficient through Fick's law. Their used technique thereby determines the product of concentration and diffusion. Their reported diffusivities were based on the evaluated solubilities of oxygen in copper by Pastorek and Rapp (1969), which shows a good agreement to calculated solubilities, see Table 3-1. More than 99.95% purity copper and Cu<sub>2</sub>O were used in the experiments.

Ransley (1939) evaluated the oxygen diffusivity in copper in the temperature range 600–950°C. The experiments were based on weight losses of an oxygen rich copper sample exposed to carbon monoxide gas. Copper with 0.41 and 0.24wt% oxygen was used, with the highest concentration of other impurities being arsenic with 0.015wt%. The carbon monoxide gas reduces surface oxides and will keep the oxygen activity low at the surface in equilibrium with the gas. This will deplete the copper on oxygen, and the rate of removal depends on three things: total oxygen content in the material, the oxygen content in solid solution, and the oxygen diffusivity. Limited information on oxygen solubility in copper was available at the time for the study. Their used oxygen contents are given in Table 3-1, and compared with the calculated solubility (Magnusson and Frisk 2013). It can be seen that the calculated solubilities are lower than what was used by Ransley, especially at low temperatures. Their reported diffusivities were recalculated based on an estimate that the permeability is proportional to the product of solubility and diffusivity. With constant permeability, new diffusion coefficients can be calculated. In the present work, their values will be shown for comparison but are not used in the evaluation of oxygen diffusivity in copper.

**Table 3-1. Reported solubilities of oxygen in copper in different experimental studies used to calculate the diffusion coefficient of oxygen in copper. All values are given in weight ppm. These solubilities are compared with calculated values based on a previous thermodynamic study of Cu-H-O-S-P system (Magnusson and Frisk 2013).**

T, °C	Ransley 1939	Országh and Bouillon 1973	Ramana Rao and Tare 1972 <sup>†</sup>	Magnusson and Frisk 2013
500		5.02, 1.53, 8.81		0.0034
600	7.1	4.07, 2.68, 5.61		0.048
700	7.8	6.67, 9.61, 5.69		0.39
800	8.7	7.79, 11.95, 18.95	4.8	2.2
840			7.8	4.0
860			9.9	5.3
900	9.7	34.95, 23.01, 34.25	15	8.8
925			20	12
950	10.5		28	16
990			40	25
1,000		36.55, 46.01, 39.42		29

<sup>†</sup> The solubilities used in the study by Ramano Rao and Tare (1972) were taken from the work by Pastorek and Rapp (1969).

Országh and Bouillon (1973) studied the total diffusing oxygen content, and the diffusion coefficient was backward calculated with assumptions on the oxygen solubility. The evaluation was made by mass-spectrometry methods, based on single crystal copper of 99.999% purity. The solubilities used in their calculations were reported, and are shown in Table 3-1. In similarity with the data by Ransley (1939), their solubilities are much higher than the calculated values. For the same reason as stated above, their data will not be used in the evaluation but are recalculated with new solubilities for comparison.

The reported data by Albert and Kirchheim (1981), Ramano Rao and Tare (1972), and Pastorek and Rapp (1969) are used to fit the temperature dependency of the oxygen diffusion coefficient in copper. This regression curve is shown in Figure 3-2, together with the experimental data. Measurements are in the temperature range 550–1,000°C. It is clearly shown that the reported oxygen diffusivity by Ransley (1939) and Országh and Bouillon (1973) deviates from the others. By recalculating their values, based on the evaluated oxygen solubility in a previous work (Magnusson and Frisk 2013) a rather good agreement is found between all different studies. The impurity diffusion coefficient of oxygen in copper is described by:

$$D_{O,Cu}^{FCC} = 1.14 \cdot 10^{-6} \exp\left(-\frac{62500}{RT}\right) \text{ m}^2/\text{s} \quad (3-2)$$

### 3.3 Cu-S

Different methods are available to evaluate sulphur diffusion in copper. The chemical properties of sulphur allows for different approaches to introduce sulphur in copper. It can be introduced both in solid state as  $^{35}\text{S}$  isotope, or by gaseous reactions. By mixing  $\text{H}_2/\text{H}_2\text{S}$  gases, the sulphur potential on the surface is well known and surface oxides can be efficiently reduced by the hydrogen content. The diffusing content of sulphur can be evaluated by both liquid scintillation counters based on annealing and sectioning of specimens, by studying the kinetics of gassing/degassing, or by studying the rate of sulphide film dissolution.

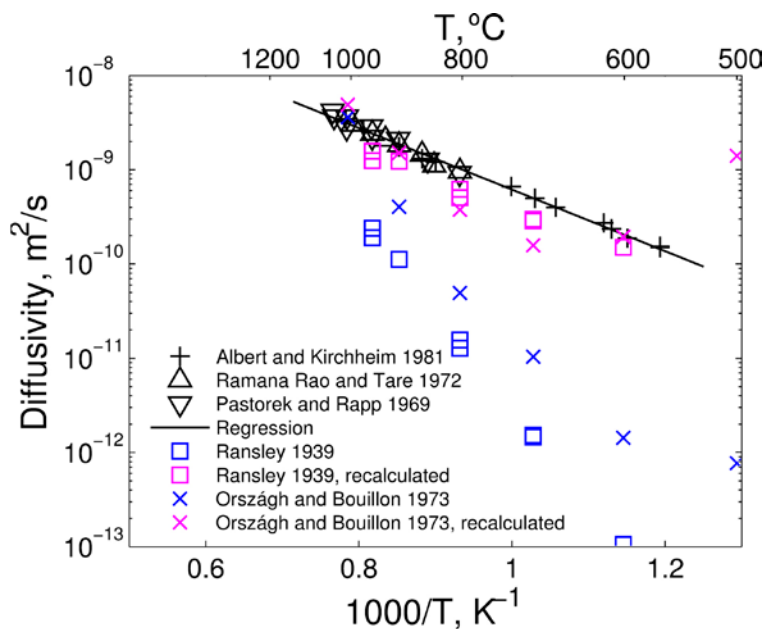


**Figure 3-2.** Evaluated oxygen diffusion coefficient in copper. References to experimental works are given in the figure. Data points presented in black colour are used in regression, blue coloured points are the original values by Ransley (1939) and Országh and Bouillon (1973), and the purple coloured data are the recalculated values using other expression for oxygen solubility in copper.

Fueki and Ouchi (1978) used copper with 99.999% purity. Copper with a thin copper sulphide film produced electrochemically was annealed for different times and at different temperatures. The thickness of the remaining sulphide film was then evaluated coulometrically and compared with the initial thickness. Based on this data the amount of diffusing sulphur was calculated. The reported sulphur solubility used in their calculation was a factor two higher compared to evaluated solubilities in a previous work (Magnusson and Frisk 2013).

Moya and Moya-Gontier (1975) used radiochemical methods to study  $^{35}\text{S}$  mobility in copper of 99.999% purity, provided by different  $\text{H}_2/\text{H}_2\text{S}$  environments. Concentration profiles were evaluated based on activity measurements of  $^{35}\text{S}$  made for both monocrystalline and polycrystalline copper. Electrolytic sectioning was used to determine the sulphur concentration profile. Further isotope evaluation was made by Ladet et al. (1978), who used single-crystal copper of 99.999% purity. The sulphur potential at the surface was held constant, and  $^{35}\text{S}$  atoms were allowed to diffuse into the material. The diffusion profile was evaluated based on activity measurements of the radiotracer after removing a part the surface with approximately  $0.5\ \mu\text{m}$  thickness.

The rates of sulphidisation and desulphidisation in  $\text{H}_2/\text{H}_2\text{S}$  environments on copper have been studied by Wang and Grabke (1970) in the temperature range  $700$  to  $1,000^\circ\text{C}$ . Thin copper foils,  $10$  to  $50\ \mu\text{m}$ , of unknown purity were used in the experiments. The sulphur content in the foil was evaluated based on resistivity changes and the time for sulphur gassing and degassing was thereby measured.

The reported diffusion coefficients in the different copper-sulphur studies have been summarised in Figure 3-3. It can be seen that the values by Ladet et al. (1978) are up to a factor of ten lower than other values. No obvious reason for this disagreement can be found. The values by Wang and Grabke (1970) lie in between the two sets of data, but showing lower activation energy (slope) in the figure. Work by Wang and Grabke on sulphur diffusion in iron, for both ferrite and austenite, shows reasonable values.

Reported literature data exist for both single-crystal and polycrystalline copper. The measurements for polycrystalline material close to  $550^\circ\text{C}$  show a minor increase in diffusion coefficient, which could be due to grain boundaries. Both Moya and Moya-Gontier (1975) and Ladet et al. (1978) have made measurements for many temperatures, at  $550$ – $1,000^\circ\text{C}$ . For this reason, the activation energy is evaluated based on these two works. The pre-exponential factor is evaluated based on all experimental data given in Figure 3-3. The corresponding Arrhenius expression for sulphur diffusion in copper is:

$$D_{S,Cu}^{FCC} = 8.1 \cdot 10^{-5} \exp\left(-\frac{183000}{RT}\right) \text{ m}^2/\text{s} \quad (3-3)$$

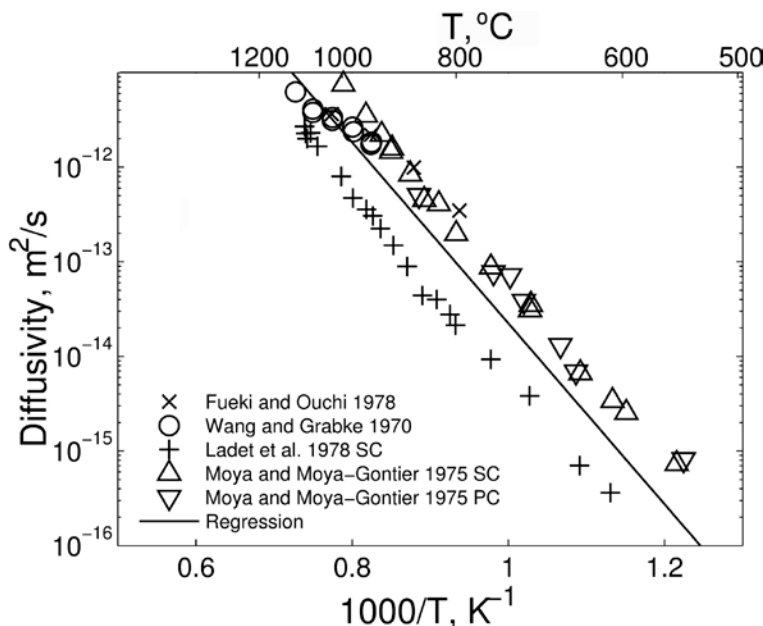


**Figure 3-3.** Evaluated sulphur diffusion coefficient in copper. References to experimental works are given in the figure. SC refers to single crystal copper, and PC polycrystalline copper.

### 3.4 Cu-P

The available literature data of phosphorus diffusion in copper are from two different works by Spindler and Nachtrieb (1976, 1978). Spindler and Nachtrieb (1976) made measurements on coarse grained polycrystalline copper and single crystal copper with 99.999% purity. In addition, the later study was on commercial purity of polycrystalline deoxidised low phosphorus copper (25 ppm phosphorus and 17 ppm oxygen). The aim with the latter study was to evaluate the influence of impurities on phosphorus diffusion in copper. The phosphorus diffusion was evaluated by radiotracer of  $^{32}\text{P}$  isotope, on annealed samples at temperature 548–1,046°C, and time periods of four hours to 18 days.

The reported phosphorus diffusivities are summarised in Figure 3-4. Data are taken for commercial purity copper from batch 3, together with the high-purity copper on both coarse grained copper and single-crystal copper. Data in the whole temperature range fall on a single line. No influence of other impurities on diffusion behaviour can be seen. The activation energy for diffusion based on this regression gave an activation energy of 138 kJ/mol. It was mentioned that the low temperature experiments showed signs of grain boundary diffusion. However, making regression only on single-crystal data in the figure yields the same activation energy. The diffusion data of phosphorus in copper gives the following expression:

$$D_{P,Cu}^{FCC} = 4.5 \cdot 10^{-7} \exp\left(-\frac{138000}{RT}\right) \text{ m}^2/\text{s} \quad (3-4)$$

### 3.5 Cu-Cu

The evaluation of self-diffusion coefficients of copper is based on radioactive measurements of either  $^{64}\text{Cu}$  or  $^{67}\text{Cu}$  isotopes. The isotope  $^{67}\text{Cu}$  has longer half-life than the more easily accessible  $^{64}\text{Cu}$  isotope (Surholt and Herzig 1997). A longer half-life allows for longer annealing times in the evaluation of concentration profiles, and thereby gives the possibility to study self-diffusion coefficients to lower temperatures. Measurements on copper self-diffusion in single crystal material are available down to 300°C, and for polycrystalline material down to 250°C.

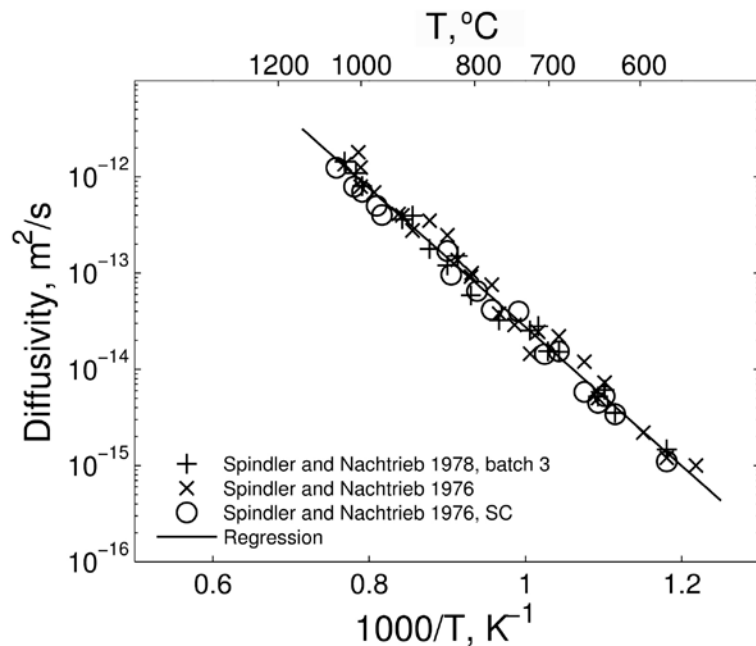


**Figure 3-4.** Phosphorus diffusion in copper, with data taken from works by Spindler and Nachtrieb. SC denotes single crystal copper.

High temperature measurements are available from older studies by Rothman and Peterson (1969) and Bartdorff et al. (1978). Rothman and Peterson made many measurements of self-diffusion coefficients in copper. Single-crystal copper with 99.999% purity was used. Both  $^{64}\text{Cu}$  and  $^{67}\text{Cu}$  isotopes were electroplated on the samples and used in the evaluations. Concentration profiles of annealed samples were evaluated based on lathe sectioning technique. Bartdorff et al. determined the self-diffusion coefficients of single-crystal copper based on 99.997% purity. Concentration profiles were evaluated based on electroplated  $^{64}\text{Cu}$  isotope, with microtome sectioning of the annealed sample.

Intermediate and low temperature measurements are mainly studied by Lam et al. (1974), Maier et al. (1973) and Maier (1977). Lam et al. studied self-diffusion in copper based on single crystals grown from 99.999% copper. Radioactive  $^{67}\text{Cu}$  isotope was used. The crystal was sectioned by anodizing technique, and the activity of the isotope was counted in a scintillation counter. Maier et al. (1973) made measurements at temperatures between 359 and 632°C on single crystal copper. The  $^{64}\text{Cu}$  isotope was used to determine the concentration profiles. Annealed material was evaluated by sputtering, with a mentioned spatial resolution down to 2 nm. Further low-temperature measurements by Maier (1977) were on single crystal copper, grown from 99.999% copper purity. The isotope  $^{64}\text{Cu}$  was used. The diffusion profiles were determined by ion-beam sputtering of material. The major part of the off-sputtered atoms were collected and measured in a scintillation counter.

The experimentally determined self-diffusion coefficients are shown in Figure 3-5. It can be seen that the different data sets fall on a single line between 300 and 1,200°C. Some deviation from this line can be seen at temperatures close to 300°C. All measurements are made on single crystal copper. Regression to self-diffusion data has been made following the temperature dependence of an Arrhenius expression. The regression is according to:

$$D_{Cu,Cu}^{FCC} = 3.0 \cdot 10^{-5} \exp\left(-\frac{202000}{RT}\right) \text{ m}^2/\text{s} \quad (3-5)$$

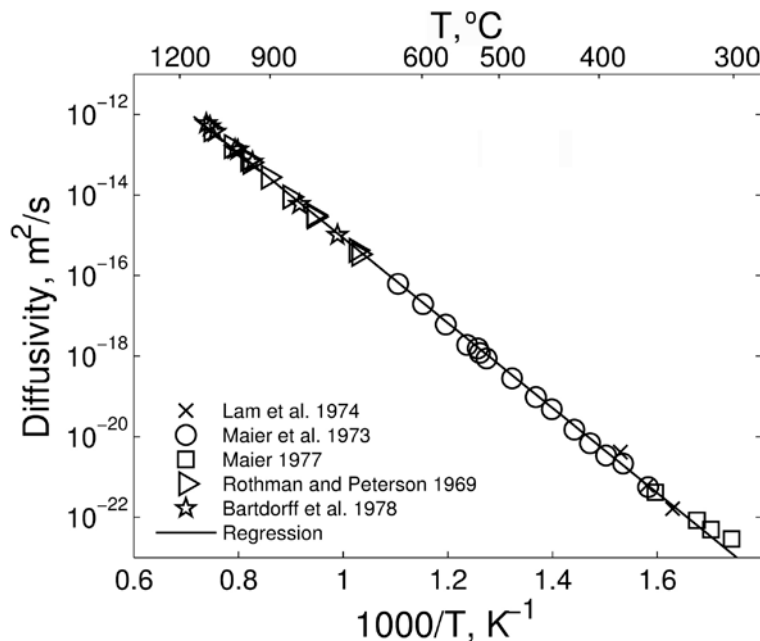


**Figure 3-5.** Self-diffusion coefficient of copper. References are given in the figure. All data are on single-crystal copper.



Hydrostatic pressure has only a little influence on diffusion rates. This is shown in Figure 3-6 for copper using experimental data from Beyeler and Adda (1968). In this work, diffusion coefficients were evaluated for single crystal copper based on the sectioning technique of annealed samples with  $^{64}\text{Cu}$  isotope. Measurements were made in the temperature range 700–990°C, and up to 10 kbar (1 GPa) hydrostatic pressure. Regression has been made to these data using the same activation energy as evaluated for the copper self-diffusion experiments previously shown in Figure 3-5. The experimental measurements at low pressure (0 kbar) agree fairly well with the other measurements on copper. For the high-pressure studies, it can be seen how higher compressive pressures decrease the diffusion coefficient. This conclusion is also in agreement with studies on other metals, for instance gold self-diffusion by Dickerson et al. (1965). The difference between atmospheric and 8 kbar hydrostatic pressures is less than a factor two. The hydrostatic pressure will thereby have only little influence on the total diffusivity.

Grain-boundary self-diffusion in copper has been studied by both Gupta (1994) and Surholt and Herzig (1997) on polycrystalline copper. The measurements by Surholt and Herzig were made on polycrystalline copper with an overall purity of 99.999%. The grain size was reported to be 200–400  $\mu\text{m}$ , based on an annealing for 24 hours at 810°C. The radioisotope  $^{64}\text{Cu}$  was used. Layers with a thickness of a few microns were removed from the specimen by a microtome, and the activity of the isotope was measured in a liquid-scintillation counter. Diffusion profiles were evaluated based on samples annealed at 447–793°C for up to 20 hours. Additional measurements on grain boundary self-diffusion of copper have been made by Gupta (1994). Copper with 99.9999% purity was used, with  $^{67}\text{Cu}$  radiotracer at temperatures of 250–650°C. The grain size was reported to be approximately 100  $\mu\text{m}$ . Sectioning of the diffusing distance into the specimen was made by microtome.

Regression has been made based on the data by Surholt and Herzig (1997), and Gupta (1994). The experimental data and the regression line are shown in Figure 3-7. The experimentally determined grain-boundary diffusion coefficients are calculated values related to lattice diffusion data. Since different lattice diffusion data were used in the two different references, the values by Gupta have been re-evaluated. Surholt and Herzig relied on data by Maier (1977), and Gupta on values by Rothman and Peterson (1969). The data by Rothman and Peterson are mainly high-temperature data (see Figure 3-5), which required extrapolation by Gupta to low temperatures in order to determine the grain boundary diffusion data. Following the procedure by Surholt and Herzig, the values by Gupta were therefore recalculated based on the same lattice diffusion data. The maximum difference at 250°C is about a factor of four, and both datasets fall on the same line. The regression line giving grain boundary self-diffusion data in copper is:

$$D_{\text{Cu,Cu}}^{\text{FCC,GB}} = 1.15 \cdot 10^{-6} \exp\left(-\frac{77200}{RT}\right) \text{ m}^2/\text{s} \quad (3-6)$$

In the calculations a grain boundary width of 0.5 nm has been used (Surholt and Herzig 1997, Gupta 1994).

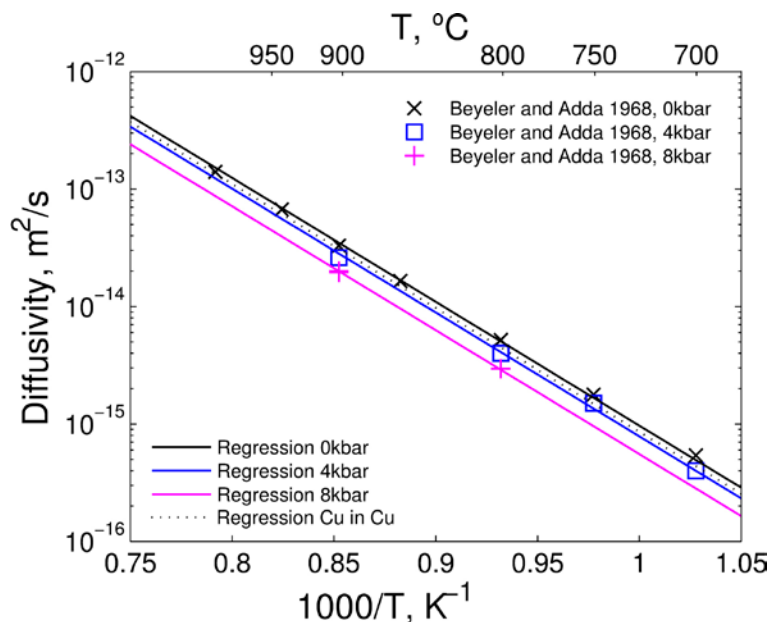


**Figure 3-6.** Self-diffusion coefficient of copper for different hydrostatic pressures. Experimental data by Beyeler and Adda (1968), and regression made to these measurements. Regression for copper self-diffusion at atmospheric pressure is shown as well, taken from Figure 3-5.

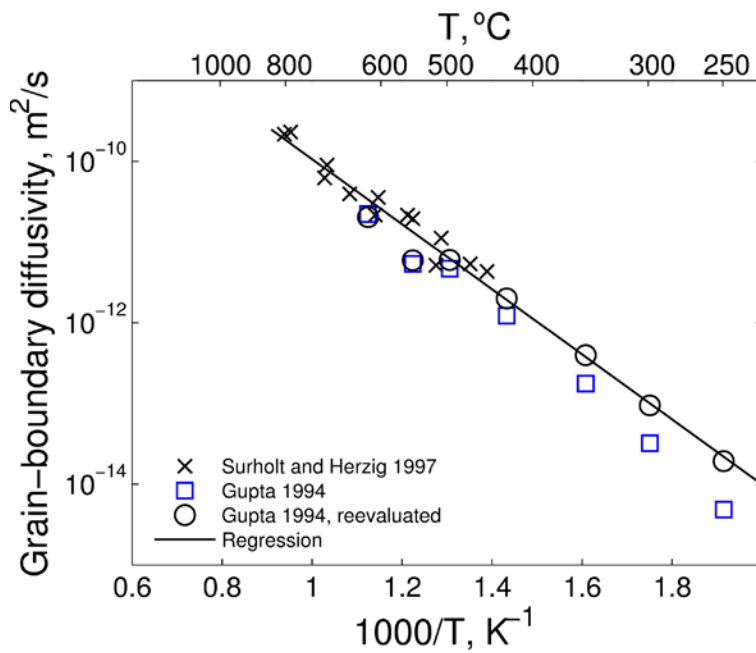


**Figure 3-7.** Evaluated grain boundary self-diffusion coefficients. The values by Gupta (1994) have been recalculated based on lattice diffusion data given by Maier (1977), which was already used by Surholt and Herzig (1997).

## 4 Extrapolation of diffusion data to low temperatures

Extrapolation of high-temperature information to low-temperature applications requires knowledge on the working mechanism of diffusion. At high temperatures the dominating diffusion mechanism for substitutional elements is lattice diffusion, and at low temperatures grain boundary diffusion. A difficulty is that there is limited amount of information available in the literature on diffusion of substitutional elements like sulphur and phosphorus in copper at low temperatures. How to extrapolate diffusion data to low temperatures will be discussed in this chapter. But first, the evaluated data of sulphur and phosphorus diffusion in copper at high temperatures will be reviewed and compared to the diffusion of other related impurity elements in copper.

Spindler and Nachtrieb (1976) commented on the low activation energy of phosphorus diffusion in copper, which was 138 kJ/mol (Equation (3-4)) compared to that of copper self-diffusion being 202 kJ/mol (Equation (3-5)). They mentioned that phosphorus diffusion in copper occurs by the same vacancy mechanism as other substitutional elements in copper. The difference in activation energy was related to theories on impurity diffusion in noble metals proposed by Lazarus (1954), and later modified by Le Claire (1962). The theory predicts that electropositive impurities should diffuse faster than other impurity atoms and that the activation energy for diffusion decreases with increasing excess valences of the impurity. The agreement to this theory is fairly good for chemical elements in the fourth period, with decreasing activation energy with increasing valence of gallium (+3), germanium (+4), arsenic (+5), and selenium (+6), as can be found in the data given in handbooks (Neumann and Tuijn 2009). However, the agreement for the third period of elements aluminium, silicon, phosphorus and sulphur is not equally good. The activation energies for phosphorus and sulphur diffusion in copper are lower than the activation energies of aluminium and silicon diffusion, which is in agreement with the suggested theory. However, the activation energy for phosphorus diffusion is much lower than that of sulphur diffusion, in disagreement with the theory.

The evaluated temperature expressions for the diffusion coefficient of sulphur Equation (3-3), phosphorus Equation (3-4), and copper in copper Equation (3-5) are shown in Figure 4-1. For comparison, the other group III elements aluminium and silicon are shown as well. Diffusion data for aluminium and silicon are taken from the handbook by Neumann and Tuijn (2009). It can be seen that the diffusivity at high temperatures are in the order Al < Si < P < S. This is in agreement with the group IV elements with increasing diffusivity with higher atomic number according to Ga < Ge < As < Se (Neumann and Tuijn 2009). It seems like the reported diffusivity of sulphur and phosphorus in copper are in the correct order and show reasonable absolute values. Since little data exists for phosphorus diffusion in copper, this remark will be accepted in the present study.

Little diffusion data for the substitutional elements sulphur and phosphorus at low temperatures can be found in the literature. The available studies are a work by Spindler and Nachtrieb (1978) on phosphorus diffusion in copper. This work was discussed in Section 3.4 as a part of the phosphorus diffusion at high temperature evaluation. In addition, a work by Moya-Gontier and Moya (1973) on sulphur diffusion in copper grain boundaries can also be found in literature. Moya and Moya-Gontier have also studied lattice diffusion of sulphur in copper as discussed in Section 3.3. A limitation in these works is the relative high temperature for grain-boundary diffusion experiments. For phosphorus in copper, the lowest temperature was 574°C and sulphur in copper 510°C. For this reason, these experimental data will be analysed and discussed, and put in relation to other grain boundary diffusing impurity elements in copper.

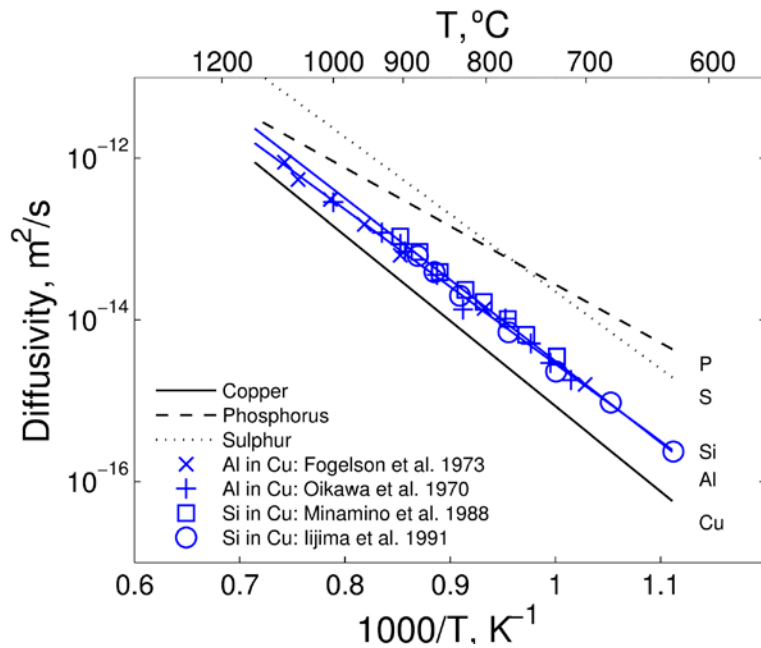


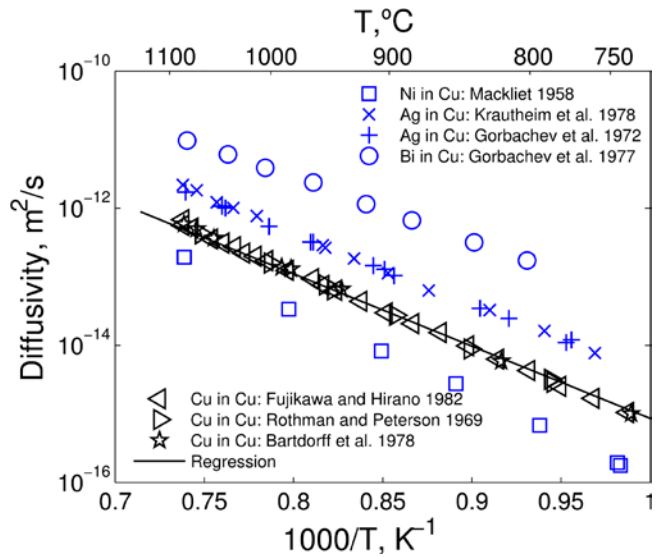
**Figure 4-1.** The evaluated regression lines for both sulphur and phosphorus diffusion in copper and copper self-diffusion are shown. Reported diffusion coefficients for the related elements aluminium and silicon in copper are shown as well. The experimental data (Fogelson et al. 1973, Oikawa et al. 1970, Minamino et al. 1988, Iijima et al. 1991) are all taken from the handbook by Neumann and Tuijn (2009).

Experimental data for impurity grain boundary diffusion in copper exists for the elements nickel, bismuth and silver (Divinski et al. 2001, 2004, 2007). A comparison of these diffusion data at high temperatures are shown in Figure 4-2a, and at low temperatures in Figure 4-2b. The low temperature diffusion data are shown for both the type-B and type-C grain boundary diffusion. The difference between these two types of diffusion is that the type-B diffusion is influenced by the lattice diffusion (see Section 2.3). For this reason, the type B diffusion is faster than the type C diffusion. The high temperature experimental data for nickel, bismuth and silver are taken from the handbook by Neumann and Tuijn (2009). It can be seen that nickel diffuses slower than copper, silver faster, and bismuth is the fastest impurity element in copper. The same relative order is found for grain boundary diffusion in the B-regime. In the C-regime, the diffusion coefficient is even lower than the copper grain boundary self-diffusion for all these elements. Similar appearance has been reported for germanium and selenium in the C-regime (Divinsky et al. 2007).

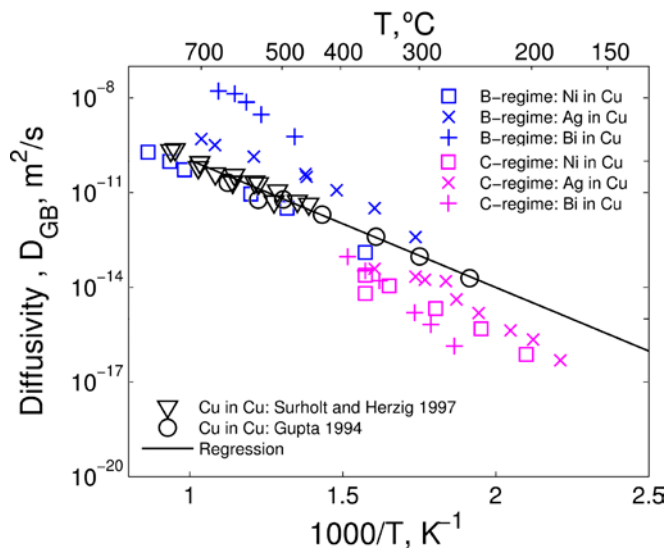
Some care should be taken when determining the transition between B-type and C-type diffusion. As discussed in Section 2.3, the temperature for the transition can be compensated by long times for diffusion. The experimental data is typically determined for experiments reaching a few days in time. At long service times, the surrounding grains can influence the grain boundary diffusion to a greater extent than the experimental setup allows. For this reason, the transition between B-type and C-type of grain boundary diffusion, as shown in Figure 4-2b, will occur at lower temperatures for longer times.

Regression has been made to diffusion data of the low-oxygen (4–17 ppm) copper grades reported by Spindler and Nachtrieb (1978). The grain boundary diffusion coefficients were evaluated for experiments at 574–703°C. Regression has been made to this data, and the diffusion coefficient of phosphorus diffusion in copper grain boundaries can be described by:

$$D_{P,Cu}^{FCC,GB} = 3.1 \cdot 10^{-4} \exp\left(-\frac{81400}{RT}\right) \text{ m}^2/\text{s} \quad (4-1)$$



a)



b)

**Figure 4-2.** Evaluated impurity diffusion coefficients of Ag, Bi and Ni in copper. a) lattice diffusion b) grain boundary diffusion. The high-temperature data references (Mackliet 1958, Krautheim et al. 1978, Gorbachev et al. 1972, Gorbachev 1977) can be found in the handbook by Neumann and Tuijn (2009). Low-temperature data references on B-regime and C-regime diffusion are from different works by Divinski et al. (2001, 2004, 2007).

In similarity, the reported diffusion data by Moya-Gontier and Moya (1973) have been used to evaluate the temperature expression for sulphur diffusion. The diffusion coefficient was evaluated at 510–852°C, and can be explained by the following relation:

$$D_{S,Cu}^{FCC,GB} = 2.0 \cdot 10^{-3} \exp\left(-\frac{81500}{RT}\right) \text{ m}^2/\text{s} \quad (4-2)$$

The grain boundary diffusion data of phosphorus and sulphur in copper is shown in Figure 4-3, and compared with copper grain boundary self-diffusion. It can be seen that phosphorus diffuses 140 times faster than copper self-diffusion in grain boundaries. The corresponding value for sulphur is 890 times faster. This difference is about the same as for bismuth diffusion in copper grain boundaries at high temperature, as shown in Figure 4-2b. These values can also be compared with high-temperature data on lattice diffusion, which was shown in Figure 4-1. At 900°C phosphorus diffuses 10 times faster than copper self-diffusion and sulphur 20 times faster. However, the reported lattice diffusion of sulphur in copper by Moya-Gontier and Moya (1975) was even higher, see Figure 3-3.

Experimental data of phosphorus and sulphur diffusion in copper below 500°C is missing in literature, and only data for type A and B kinetics of boundary diffusion exists. As previously shown in Figure 4-2, the impurity diffusion in regime B is typically much faster than self-diffusion rates. The impurity diffusion rate is much lower in regime C. This is due to less contribution from the surrounding grains with less segregation of the impurity. This will probably occur for phosphorus and sulphur diffusion in copper as well, however, no experimental data to prove this exists. In this work, the evaluated expressions for phosphorus and sulphur diffusion in copper grain boundaries (Equations (4-1) and (4-2)) will be used to calculate the diffusion distance of sulphur and phosphorus in the grain boundaries. This will yield estimates at the upper limit of possible diffusion lengths of these impurities in the grain boundaries.

The effective diffusivity of H, O, S, P and Cu in Cu at low temperatures is shown in Figure 4-4. Hydrogen and oxygen is assumed to diffuse as interstitial elements at low temperatures. In the case of hydrogen, it has been experimentally studied down to room temperature. Oxygen measurements are down to 550°C, and lower temperatures are extrapolations. Copper grain-boundary diffusion has been studied down to 250°C. Sulphur and phosphorus grain boundary diffusion are given in Equations (4-1) and (4-2), based on type-A or type-B grain boundary diffusion. At room-temperature with type-C diffusion, the diffusion coefficient of these elements should be closer to the copper self-diffusion rate. The interstitial elements diffuse through the whole materials, and the substitutional elements diffuse in the grain boundaries included in the definition of effective diffusivity, see Equation (2-1).

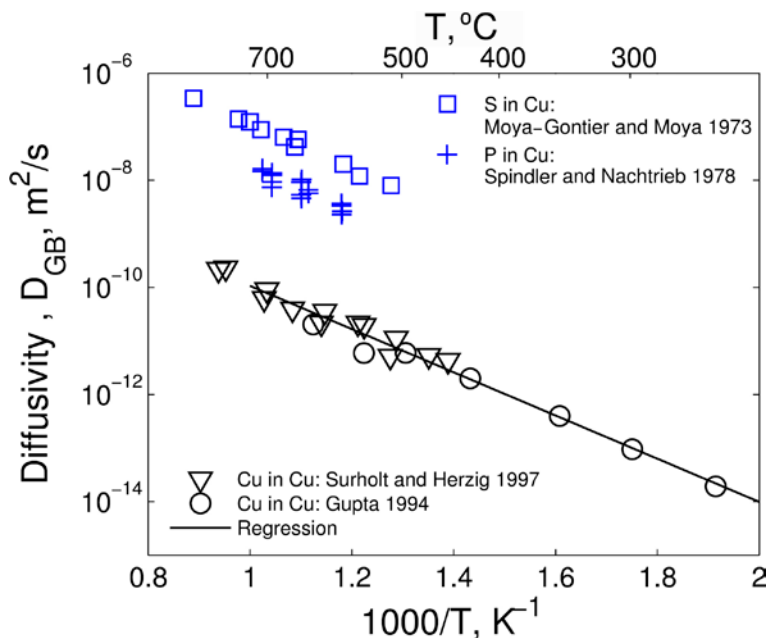


**Figure 4-3.** Reported grain boundary diffusion coefficients of phosphorus in copper by Spindler and Nachtrieb (1978), and sulphur in copper by Moya-Gontier and Moya (1973). These values are compared with copper self-diffusion coefficients.

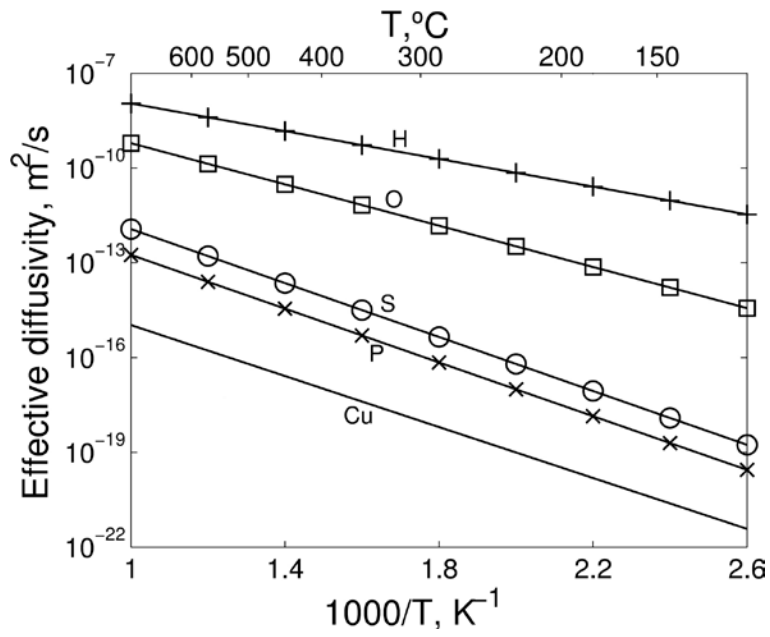


**Figure 4-4.** Effective diffusion coefficient for copper self-diffusion, and for impurity diffusion of phosphorus, sulphur, oxygen and hydrogen.

## 5 Relating time and temperature to a diffusion distance

### 5.1 Grain boundary diffusion and lattice diffusion

The time and temperature dependence of the different regimes of diffusion can be evaluated, as shown in Figure 5-1 (Herzig and Mishin 2005). The grain boundary thickness  $\delta$  has been given its typical value of 0.5 nm, and the grain size  $d_{GB}$  was given a typical value of 100  $\mu\text{m}$ . The time relation indicates that for slow processes or long service times the lattice diffusion can influence the total diffusivity even at low temperatures. At low temperatures, below 100°C, copper self-diffusion will be entirely located at grain boundaries even for service times up to 100,000 years. The lattice diffusivity of sulphur and phosphorus is slightly higher than the copper self-diffusion and the transition between regime-B and regime-C will be closer to service conditions. In this work, the B-type diffusivities of phosphorus and sulphur will be considered. Extrapolation of diffusion data based on the B-type of diffusion gives higher diffusivity than that based on the C-type of diffusion.

High-temperature creep is a temperature activated mechanism showing similar activation energy as self-diffusion. This has been shown for many different metals by Sherby and Weertman (1979). The high-temperature creep is based on dislocation climb, which relies on the availability of vacancies for dislocation movement. The presence of high-temperature creep is an indication of where any vacancy mobility within grains can be expected. By using the experimentally determined creep data for OFP-Cu by Sandström and Andersson (2008), and defining high-temperature creep where the creep exponent takes a value of 4 (Kassner and Pérez-Prado 2000), the time-temperature relation for high temperature creep can be determined as illustrated in Figure 5-1. The line indicates that at higher temperatures or longer times a vacancy assisted dislocation motion can be expected. This is in agreement with the estimation of when lattice diffusivity can be of importance.

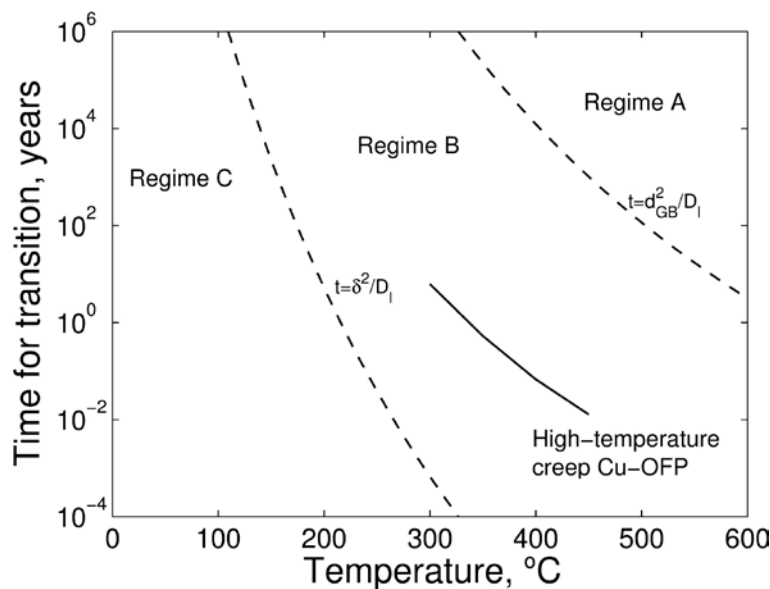


**Figure 5-1.** Time and temperature where different types of diffusion mechanisms will control the overall mass transport in the material. The indication of high-temperature creep is the shortest time and lowest temperature where high-temperature creep of OFP-Cu can be expected based on experimentally evaluated creep data (Sandström and Andersson 2008).



## 5.2 Sulphur and phosphorus diffusion

The time needed for sulphur and phosphorus to diffuse a distance of 1 nm or 1  $\mu\text{m}$  within the grain, as evaluated based on lattice diffusion data, is shown in Figure 5-2 and compared with copper self-diffusion. Based on these estimates it can be concluded that practically no diffusion will occur within the grains at low temperature, even for very long time periods. As an approximation, a temperature above 200°C is needed for any significant lattice diffusion.

The times needed for sulphur, phosphorus and copper atoms to diffuse a distance of 5 cm and 50  $\mu\text{m}$  in the grain boundaries are shown in Figure 5-3. These times are calculated based on the determined diffusivities for grain boundary diffusion. It is not the effective diffusivity defined in Equation (2-1), but instead the maximum diffusion distance one could expect at these conditions in the grain boundaries. It can be seen that sulphur and phosphorus can diffuse on the order of 5 cm in grain boundaries during a time period of 100,000 years at room temperature. Sulphur and phosphorus can diffuse a typical grain distance (50  $\mu\text{m}$ ) in less than one year at temperatures above 40°C.

The calculated diffusion distance is an estimate of the possible distance a diffusing atom might reach. In practice, the solubility of sulphur in copper is extremely low at low temperatures (Magnusson and Frisk 2013), and the total content of permeating sulphur will be very low. On the other hand, the phosphorus content is in solid solution at low temperatures (Magnusson and Frisk 2013) since the solubility limit of copper phosphide  $\text{Cu}_3\text{P}$  is much higher than the used phosphorus content in OFP-Cu. In the case of phosphorus, the diffusion distance can be a good estimate of the mobility of phosphorus at low temperatures.

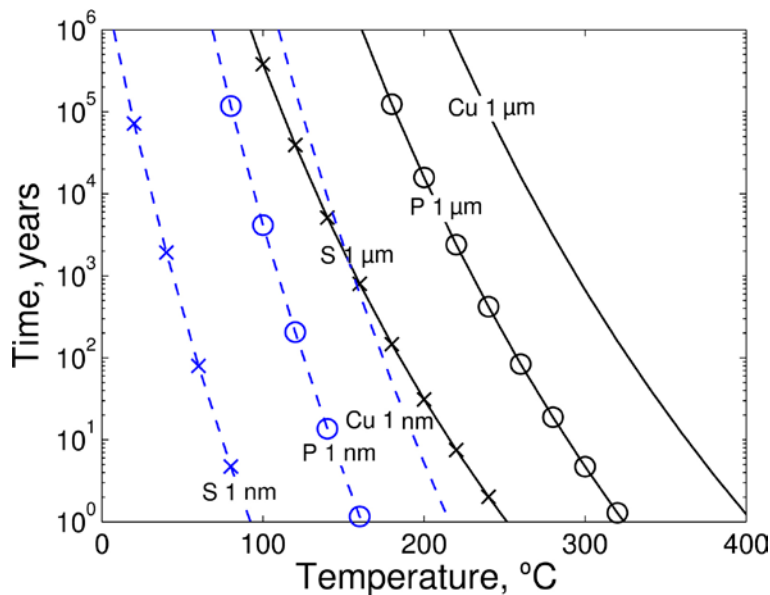


**Figure 5-2.** Calculated time needed for sulphur, phosphorus and copper to diffuse 1 nm (blue, dashed line) and 1  $\mu\text{m}$  (black, solid line) within the grains based on lattice diffusion data extrapolated from high temperatures.

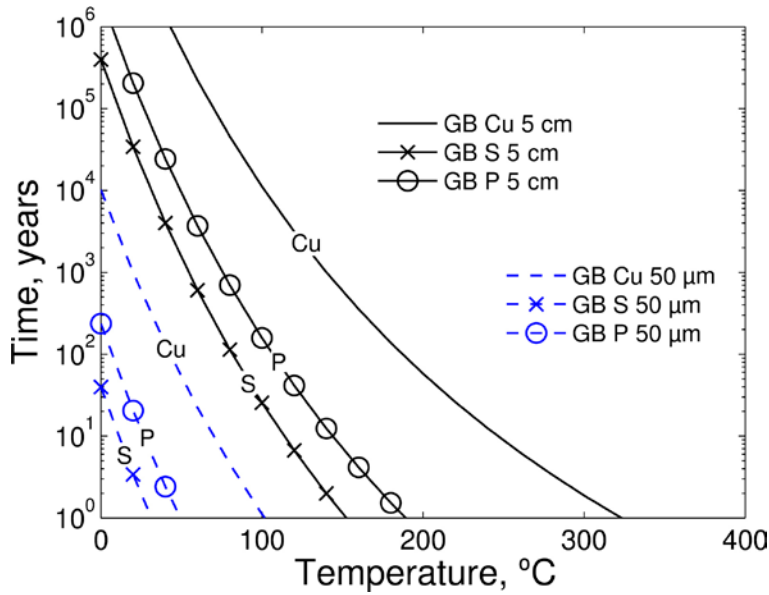


**Figure 5-3.** Calculated time needed for sulphur, phosphorus, and copper to diffuse 5 cm (black solid lines) and 50  $\mu\text{m}$  (blue dashed lines) in grain boundaries.

### 5.3 Hydrogen and oxygen diffusion

The times needed for hydrogen and oxygen to diffuse a distance of 1 mm and 5 cm are shown in Figure 5-4. Both these elements are treated as interstitially diffusing elements, and described by single Arrhenius expressions in the whole temperature range. In the case of hydrogen, this is verified for low temperatures. In the case of oxygen, the low temperature calculations rely on extrapolations from high temperatures. In similarity with sulphur, oxygen will have an extremely low solubility in solid solution in the presence of copper phosphates or copper oxides (Magnusson and Frisk 2013). The total mass transfer of oxygen will therefore be low, even though the mobility of the elements is relatively high.

A diffusing distance of 5 cm is shown as well, based on the thickness of the copper canister material. It can be shown that the oxygen atom will not be able to diffuse this distance during service conditions. On the other hand, the highly mobile hydrogen atom will.

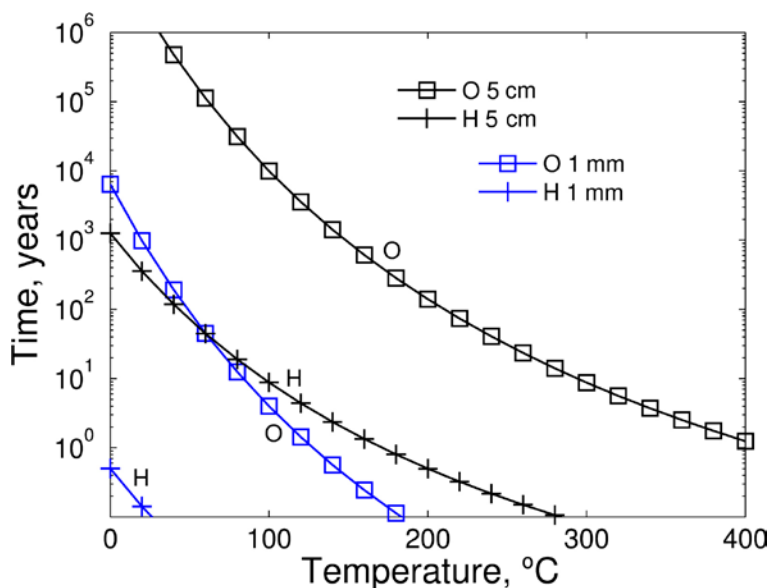


**Figure 5-4.** Calculated time needed for oxygen and hydrogen to diffuse 1 mm (black lines) and 5 cm (blue lines).

The characteristic of the highly mobile hydrogen atom makes it possible to experimentally study its mobility down to room-temperature. The content of hydrogen permeating through a copper foil has been evaluated in many studies. By using hydrogen isotopes it is possible to measure low concentrations of radioactive isotopes in scintillation counters. Experimental data are shown in Figure 5-5, together with regression line and calculated permeability made in this work. Older experimental data are taken from a summary by Butrymowicz et al. (1975), and newer works are by Caskey et al. (1976) and Horinouchi et al. (2013). The hydrogen permeability can be described by the following relation:

$$P_{H,Cu}^{FCC} = 4.5 \cdot 10^{-4} \exp\left(-\frac{84320}{RT}\right) \text{ mol H}_2/\text{m}\cdot\text{s}\cdot\text{atm}^{0.5} \quad (5-1)$$

The calculated model values are an estimate based on Fick's law given in Equation (2-2). It has been assumed that a steady-state concentration profile has been reached. The concentration gradient is therefore the hydrogen content on the high-pressure side minus the hydrogen content on the vacuum side (put to zero) divided with the distance unit length. The concentration of hydrogen is in this case given in mole H<sub>2</sub> per unit volume. The hydrogen content on the high-pressure side has been calculated based on the thermodynamic evaluation made in previous work (Magnusson and Frisk 2013). The total flux of hydrogen will then be proportional to the diffusion coefficient (Equation (3-1)) times the concentration gradient of hydrogen. The calculated hydrogen solubility will follow Sievert's law, relating the solubility to the square root of the pressure. This relation has been verified for copper for a range of temperatures and pressures, as discussed in previous work (Magnusson and Frisk 2013). The low temperature measurements by Caskey et al. shown in Figure 5-5 are for tritium gas at 69 MPa pressure. The high pressure makes it possible to increase the rate of hydrogen permeation at low temperatures.

The model slightly underestimates the permeability. At 75°C the difference is a factor of ten between regression line and model line. It seems to be a systematic error, possibly due to incorrect activation energy for diffusion or solubility. The diffusivity evaluated in Section 3.1 is quite well documented down to room temperature and should be accurate. It is more difficult to accurately evaluate the solubility of hydrogen in copper at low temperatures. The present thermodynamic description relies on extrapolation of high-temperature measurements from 500°C and higher (Magnusson and Frisk 2013). It is possible that the solubility could be a little higher in FCC-copper, which would give better predictions of the hydrogen permeability at low temperatures. Nevertheless, the overall agreement is quite good to the permeability data. A strong temperature dependency of the permeability can be seen. This is due to the fact that both the diffusivity and solubility of hydrogen in copper rapidly increase with temperature.

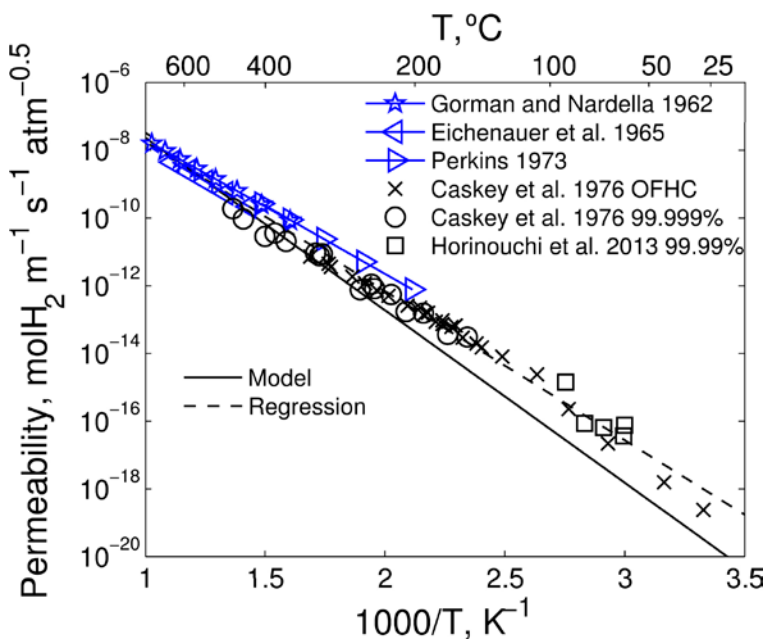


**Figure 5-5.** Experimental measurements on hydrogen permeability in copper. Older references before 1975 are taken from Butrymowicz et al. (1975), these are Gorman and Nardella (1962), Eichenauer (1965), and Perkins (1973). Additional experimental data are from Caskey et al. (1976) and Horinouchi et al. (2013). Regression has been made to all experimental data, and is compared with model values.

## 6 Discussion

In this work, the diffusion coefficients describing copper self-diffusion and hydrogen, oxygen, sulphur and phosphorus impurity diffusion have been evaluated. For the substitutional elements copper, sulphur and phosphorus, their low-temperature and high-temperature diffusion behaviours have been studied. Oxygen and hydrogen as interstitially diffusing elements have been described with the same mechanism at both high and low temperatures. Based on this information, the mobility of all these elements has been analysed for different temperature regimes and time scales. These results will be now discussed in this chapter.

Copper, sulphur and phosphorus atoms within grains at low temperatures will appear nearly immobile for long times at low temperatures. Calculations using lattice diffusion data yields less than 1 nm diffusion distance within grains at room temperature. To some extent, the atoms that are connected to a grain boundary can appear slightly mobile. By using the grain boundary diffusion data at room temperature a typical length scale of 5 cm diffusion in grain boundaries can be expected for a time period of 100,000 years. This should be seen as an upper limit in diffusing distance, based on the evaluated grain boundary diffusion data at 500–700°C (type A and type B kinetics). Impurity diffusion at room temperature for copper will probably be even slower, comparable to grain boundary self-diffusion according to type C kinetics that requires more than a million years to diffuse 5 cm.

Diffusion of smaller atoms in lattice through interstitial diffusion will proceed much faster. The small hydrogen atom will be able to diffuse through the copper shell material, and the 5 cm diffusion distance is reached in less than 1,000 years. Oxygen is diffusing relatively fast compared to the substitutional elements, but much slower than hydrogen. Calculations have shown that the oxygen atom will not be able to diffuse through the copper shell material. In addition, it will have an extremely low solubility forming oxides rather than diffusing through the material.

The evaluation of diffusion coefficients made in this work has highlighted the importance to separate between direct measurements of diffusion coefficients, and indirect measurements for instance by permeability experiments. Permeability studies require information on the solubility of the element in order to calculate its diffusivity. In the case of oxygen, which has a very low solubility at low temperatures, this has given completely different estimates of the oxygen diffusion coefficient. By using a previously evaluated thermodynamic description for oxygen solubility in copper, the reported diffusion data for oxygen can be understood.

Hydrogen is a relatively mobile atom even at low temperatures, and data from permeability experiments down to room temperature can be found in the literature. Permeability calculations require information on the solubility. The experimentally determined hydrogen content in OFP-copper is much higher than the calculated content in solid solution. Concentrations as high as 0.5 weight ppm are common. The hydrogen solubility has been previously studied as a part of the thermodynamic evaluation of the Cu-H-O-S-P system (Magnusson and Frisk 2013). The calculated soluble content of hydrogen in FCC-copper was much lower than what is measured. The difference is up to  $10^7$  times lower at room temperature. However, crystalline defects such as cavities, dislocations, and grain boundaries are not part of the thermodynamic model, and these defects will be suitable trapping sites for the small hydrogen atom. Nevertheless, the calculated soluble hydrogen content is still an important quantity. It has been showed in this work how the calculated hydrogen content in solid solution can be used together with the evaluated hydrogen diffusivity to determine the permeability of hydrogen. This has been shown to be valid both at high temperatures and down to room temperature. It can therefore be concluded that it will only be the hydrogen in solid solution that takes part of the mass-transfer and not the total hydrogen content trapped in crystalline defects.

The low content of diffusing hydrogen has also been demonstrated in hydrogen charging/degassing experiments (Martinsson and Sandström 2012). Hydrogen charging with high hydrogen activity gives high hydrogen content close to the surface, although the content decreases rapidly with distance. Modelling the hydrogen transport based on the measured hydrogen content would give a very rapid mass-transport, which is not observed in the permeability experiments. This again demonstrates that only a minor part of the hydrogen content is taking part of the mass-transport.

In a similar manner, the process of degassing will be slow due to the low content of hydrogen in solid solution. The process of degassing will be even more complicated due to the strong interaction between oxygen and hydrogen that will impede the kinetics (Caskey et al. 1976, Horinouchi et al. 2013). Hydrogen degassing at room-temperature will probably proceed faster if the surface oxides would first be reduced. Reduction of copper oxides has been studied in hydrogen gas mixtures corresponding to hydrogen activity close to unity relative 1 atm H<sub>2</sub> gas. CuO reduction takes place at 200–300°C (Jelić et al. 2011), and Cu<sub>2</sub>O at higher temperatures due to its higher stability at 350–450°C (Tilliander et al. 2006). These reduction temperatures will be lower for higher hydrogen activities, for instance hydrogen charged copper.

Both the hydrogen solubility and hydrogen diffusivity has been independently evaluated and studied in different works. Expressions for both these quantities have been verified in this work by considering the permeability data of hydrogen in copper. When considering the experimental difficulties in measuring solvable hydrogen in copper at low temperatures, and its diffusivity at room temperature, the agreement to the permeability data is quite good. The relation between permeability and solubility and between solubility and hydrogen pressures or activities make it possible to make mass transfer calculations for hydrogen when applying different boundary conditions for the hydrogen content. These boundary conditions can be defined by corrosion processes, gassing/degassing, or electrochemical charging of hydrogen.

## 7 Conclusions

A kinetic study on the self-diffusion rate of copper and impurity diffusion rate of hydrogen, oxygen, sulphur, and phosphorus in copper has been made. Different mechanisms for diffusion have been evaluated. Diffusion distances for the different elements have been calculated, and their possible influence during service conditions has been discussed. Some general conclusions about the different elements are:

Hydrogen diffusion in OFP-Cu can be explained by a single Arrhenius expression in the whole temperature range down to room temperature. It is a mobile element, being able to diffuse more than 5 cm during 1,000 years. As an interstitially diffusing element, it will be able to diffuse through the grains and not only in the grain boundaries. By combining previously evaluated hydrogen solubility with diffusivity determined in this work, reported data on hydrogen permeability can be explained. This verifies the evaluated expressions for hydrogen. This also verifies that only hydrogen in solid solution takes part in the mass transport.

Oxygen is modelled as an interstitially diffusing element. Experimental data in the literature show some scatter, but can be explained if a correct solubility of oxygen in copper is taken into consideration. Diffusion data exist down to 550°C. The oxygen atom is fairly mobile, but will not be able to diffuse through the canister thickness. It should be reminded that the solubility of oxygen in copper is extremely low, and there will not be any measurable mass transport of oxygen in copper.

The sulphur diffusion rate has been shown to be in close connection with copper self-diffusion data. Lattice diffusion data at 900°C gives nearly 20 times faster diffusion than copper self-diffusion. Grain boundary diffusion data at 500–700°C indicates nearly 900 times faster diffusion compared to copper self-diffusion. Based on this diffusion data, the diffusion distance at room temperature has been calculated to 5 cm for 100,000 years. However, impurity diffusion at low temperature is often slower than copper self-diffusion, and the calculated diffusion distance should be seen as an upper limit estimate. In similarity with oxygen, sulphur has a very low solubility forming sulphides in the material. For this reason, significant sulphur diffusion will never take place.

Phosphorus diffusion deviates from other substitutional diffusing elements by showing lower activation energy, although its absolute values are still close to copper self-diffusion. At 900°C it is approximately 10 times the copper self-diffusion. Phosphorus diffusion has been experimentally studied down to 575°C. Grain boundary diffusion data shows 140 times faster diffusion than copper self-diffusion. A typical diffusion distance in grain boundaries is 5 cm during 1,000 000 years, or one grain size (50 µm) for one year at 40°C. In similarity with sulphur, this should be seen as an upper limit in distance. Practically no phosphorus diffusion will take place within the grains at low temperatures. In opposite to sulphur, phosphorus has a fairly high solubility in FCC-copper and the total mass transport can be relatively high.

Copper self-diffusion has been well documented for single-crystal materials down to approximately 300°C, and polycrystalline material down to 250°C. The copper self-diffusion rate can be used as an estimate on the diffusion rate of substitutional elements in copper, when other data are missing. The vacancy controlled self-diffusion (lattice diffusion) shows agreement to when vacancy controlled creep (high-temperature creep) can be expected for OFP-Cu.

## References

SKB's (Svensk Kärnbränslehantering AB) publications can be found at [www.skb.se/publications](http://www.skb.se/publications).

- Albert E, Kirchheim R, 1981.** Diffusivity of oxygen in copper. *Scripta metallurgica* 15, 673–677.
- Andersson-Östling H C M, Sandström R, 2009.** Survey of creep properties of copper intended for nuclear waste disposal. SKB TR-09-32, Svensk Kärnbränslehantering AB.
- Bartdorff D, Neumann G, Reimers P, 1978.** Self-diffusion of  $^{64}\text{Cu}$  in copper single crystals. Monovacancy and divacancy contributions. *Philosophical Magazine A* 38, 157–165.
- Beyeler M, Adda Y, 1968.** Détermination des volumes d'activation pour la diffusion des atomes dans l'or, le cuivre et l'aluminium. *Journal de Physique* 29, 345–352. (In French.)
- Butrymowicz D B, Manning J R, Read M E, 1975.** Diffusion in copper and copper alloys. Part III. Diffusion in systems involving elements of the groups IA, IIA, IIIB, IVB, VB, VIB, and VIIB. *Journal of Physical and Chemical Reference Data* 4, 177–249.
- Caskey G R, Dexter A H, Holzworth M L, Louthan M R, Derrick R G, 1976.** The effect of oxygen on hydrogen transport in copper. *Corrosion* 32, 370–374.
- Dickerson R H, Lowell R C, Tomizuka C T, 1965.** Effect of hydrostatic pressure on the self-diffusion rate in single crystals of gold. *Physical Review* 137, A613–A619.
- Divinski S, Lohmann M, Herzig C, 2001.** Ag grain boundary diffusion and segregation in Cu: measurements in the types B and C diffusion regimes. *Acta Materialia* 49, 249–261.
- Divinski S, Lohmann M, Herzig C, 2004.** Grain boundary diffusion and segregation of bi in Cu: radiotracer measurements in B and C diffusion regimes. *Acta Materialia* 52, 3973–3982.
- Divinski S, Ribbe J, Schmitz G, Herzig C, 2007.** Grain boundary diffusion and segregation of Ni in Cu. *Acta Materialia* 55, 3337–3346.
- Eichenauer W, Pebler A, 1957.** Messung des Diffusionskoeffizienten und der Löslichkeit von Wasserstoff in Aluminium und Kupfer. *Zeitschrift für Metallkunde* 48, 373–378.
- Eichenauer W, Löser W, Witte H, 1965.** Löslichkeit und Diffusionsgeschwindigkeit von Wasserstoff und Deuterium in Einkristallen aus Nickel und Kupfer. *Zeitschrift für Metallkunde* 56, 287–293.
- Fueki K, Ouchi Y, 1978.** Solubility and diffusion coefficient of sulfur in copper. *Bulletin of the Chemical Society of Japan* 51, 2234–2236.
- Gorman J K, Nardella W R, 1962.** Hydrogen permeation through metals. *Vacuum Science Technology* 12, 19–24.
- Gupta D, 1994.** Comparative Cu diffusion studies in advanced metallizations of Cu and Al-Cu based thin films. In *Proceedings of the 1994 MRS Spring Meeting - Symposium B*. Pittsburgh, PA: Materials Research Society. (Materials Research Society Symposium Proceedings 337), 209–215.
- Gupta D, Campbell D R, Ho P S, 1978.** Grain boundary diffusion. In Poate J M, Tu K N, Mayer J W (eds). *Thin films: interdiffusion and reactions*. New York: Wiley.
- Harrison L G, 1961.** Influence of dislocations on diffusion kinetics in solids with particular reference to the alkali halides. *Transactions of the Faraday Society* 57, 1191–1199.
- Hart E W, 1957.** On the role of dislocations in bulk diffusion. *Acta Metallurgica* 5, 597.
- Herzig C, Mishin Y, 2005.** Grain boundary diffusion in metals. In Heitjans P, Kärger J (eds). *Diffusion in condensed matter: methods, materials, models*. Berlin: Springer-Verlag, 336–363.
- Horinouchi H, Shinohara M, Otsuka T, Hashizume K, Tanabe T, 2013.** Determination of hydrogen diffusion and permeation coefficients in pure copper at near room temperature by means of tritium tracer techniques. *Journal of Alloys and Compounds* 580, S73–S75.
- Ishikawa T, McLellan R B, 1985.** The diffusivity of hydrogen in copper at low temperatures. *Journal of Physics and Chemistry of Solids* 46, 445–447.

- Jelić D, Tomić-Tucaković B, Mentus S, 2011.** A kinetic study of copper(II) oxide powder reduction with hydrogen, based on thermogravimetry. *Thermochimica Acta* 521, 211–217.
- Kassner M E, Pérez-Prado M-T, 2000.** Five-power-law creep in single phase metals and alloys. *Progress in Materials Science* 45, 1–102.
- Katz L, Guinan M, Borg R J, 1971.** Diffusion of H<sub>2</sub>, D<sub>2</sub>, and T<sub>2</sub> in single-crystal Ni and Cu. *Physical Review B* 4, 330–341.
- Ladet J, Aufray B, Moya F, 1978.** Sulphur diffusion in silver and copper single crystals. *Metal Science* 12, 195–197.
- Lam N Q, Rothman S J, Nowicki L J, 1974.** Self-diffusion in copper at low temperatures. *Physica Status Solidi (a)* 23, K35–K38.
- Lazarus D, 1954.** Effect of screening on solute diffusion in metals. *Physical Review* 93, 973–976.
- Le Claire A D, 1962.** On the theory of impurity diffusion in metals. *Philosophical Magazine* 7, 141–167.
- Magnusson H, Frisk K, 2013.** Thermodynamic evaluation of Cu-H-O-S-P system. Phase stabilities and solubilities for OFP-copper. SKB TR-13-11, Svensk Kärnbränslehantering AB.
- Maier K, 1977.** Self-diffusion in copper at “low” temperatures. *Physica Status Solidi (a)* 44, 567–576.
- Maier K, Bassani C, Schüle W, 1973.** Self-diffusion in copper between 359 and 632°C. *Physics Letters* 44A, 539–540.
- Martinsson Å, Sandström R, 2012.** Hydrogen depth profile in phosphorus-doped, oxygen-free copper after cathodic charging. *Journal of Materials Science* 47, 6768–6776.
- Mishin Y, Herzig C, Bernardini J, Gust W, 1997.** Grain boundary diffusion: fundamentals to recent development. *International Materials Reviews* 42, 155–178.
- Moya F, Moya-Gontier G E, 1975.** Étude de la ségrégation intergranulaire du soufre dans le cuivre. *Journal de Physique C4*, 157–164. (In French.)
- Moya-Gontier G E, Moya F, 1973.** Influence de la segregation aux joints sur la diffusion intergranulaire du soufre dans le cuivre. *Acta Metallurgica* 21, 701–708.
- Murch G E, Nowick A S, 1984.** Diffusion in crystalline solids. New York: Academic Press.
- Murch G E, Rothman S J, 1985.** Grain Boundary diffusion at high densities of grain boundaries. *Diffusion and Defect Data* 42, 17–28.
- Neumann G, Tuijn C, 2009.** Self-diffusion and impurity diffusion in pure metals: handbook of experimental data. Amsterdam: Pergamon.
- Országh J, Bouillon F, 1973.** Diffusion de l’oxygène dans le cuivre monocristallin. *Mémoires Scientifiques de la Revue de Métallurgie* 70, 319–325. (In French.)
- Pastorek R L, Rapp R A, 1969.** The solubility and diffusivity of oxygen in solid copper from electrochemical measurements. *Transactions of the Metallurgical Society of AIME* 245, 1711–1720.
- Perkins W G, 1973.** Permeation and outgassing of vacuum materials. *Journal of Vacuum Science Technology* 10, 543–556.
- Perkins W G, Begeal D R, 1972.** Permeation and diffusion of hydrogen in ceramvar, copper and ceramvar-copper laminates. *Berichte der Bunsengesellschaft für physikalische Chemie* 76, 863.
- Ramana Rao A V, Tare V B, 1972.** Diffusion coefficient of oxygen in solid copper by the steady state current method using a solid electrolyte. *Zeitschrift für Metallkunde* 63, 70–73.
- Ransley C E, 1939.** The diffusion of oxygen in copper. *Journal of the Institute of Metals* 65, 147–172.
- Rothman S J, Peterson N L, 1969.** Isotope effect and divacancies for self-diffusion in copper. *Physica Status Solidi (b)* 35, 305–312.
- Sakamoto Y, Takao K, 1982.** The electrochemical determination of diffusivity and solubility of hydrogen in copper. *Journal of the Japan Institute of Metals* 46, 285–290.



- Sandström R, Andersson H C M, 2008.** The effect of phosphorus on creep in copper. *Journal of Nuclear Materials* 372, 66–75.
- Sherby O D, Weertman J, 1979.** Diffusion-controlled dislocation creep: a defense. *Acta Metallurgica* 27, 387–400.
- SKB, 2006.** Kapsel för använt kärnbränsle. Konstruktionsförutsättningar. SKB R-06-02, Svensk Kärnbränslehantering AB. (In Swedish.)
- SKB, 2009.** Design premises for a KBS-3V repository based on results from the safety assessment SR-Can and some subsequent analyses. SKB TR-09-22, Svensk Kärnbränslehantering AB.
- SKB, 2010a.** Corrosion calculations report for the safety assessment SR-Site. SKB TR-10-66, Svensk Kärnbränslehantering AB.
- SKB, 2010b.** Design, production and initial state of the canister. SKB TR-10-14, Svensk Kärnbränslehantering AB.
- Spindler P, Nachtrieb K, 1976.** Diffusion of phosphorus in copper. *Physica Status Solidi (a)* 37, 449–456.
- Spindler P, Nachtrieb K, 1978.** Lattice and grain-boundary diffusion of phosphorus in commercially-pure copper. *Metallurgical Transactions* 9A, 763–767.
- Surholt T, Herzig C, 1997.** Grain boundary self-diffusion in Cu polycrystals of different purity. *Acta Materialia* 45, 3817–3823.
- Tilliander U, Ragnhild A E, Seetharaman S, 2006.** Kinetics studies of hydrogen reduction of  $\text{Cu}_2\text{O}$ . *Zeitschrift für Metallkunde* 91, 72–78.
- Wang S J, Grabke H J, 1970.** Untersuchungen der Diffusion des Schwefels in Metallen bei der Reaktion in  $\text{H}_2\text{S}$ - $\text{H}_2$ -Gemischen. *Zeitschrift für Metallkunde* 61, 597–603. (In German.)
- Wu R, Sandström R, Jin L-Z, 2013.** Creep crack growth in phosphorus alloyed oxygen free copper. *Materials Science and Engineering A* 583, 151–160.